Figure S1

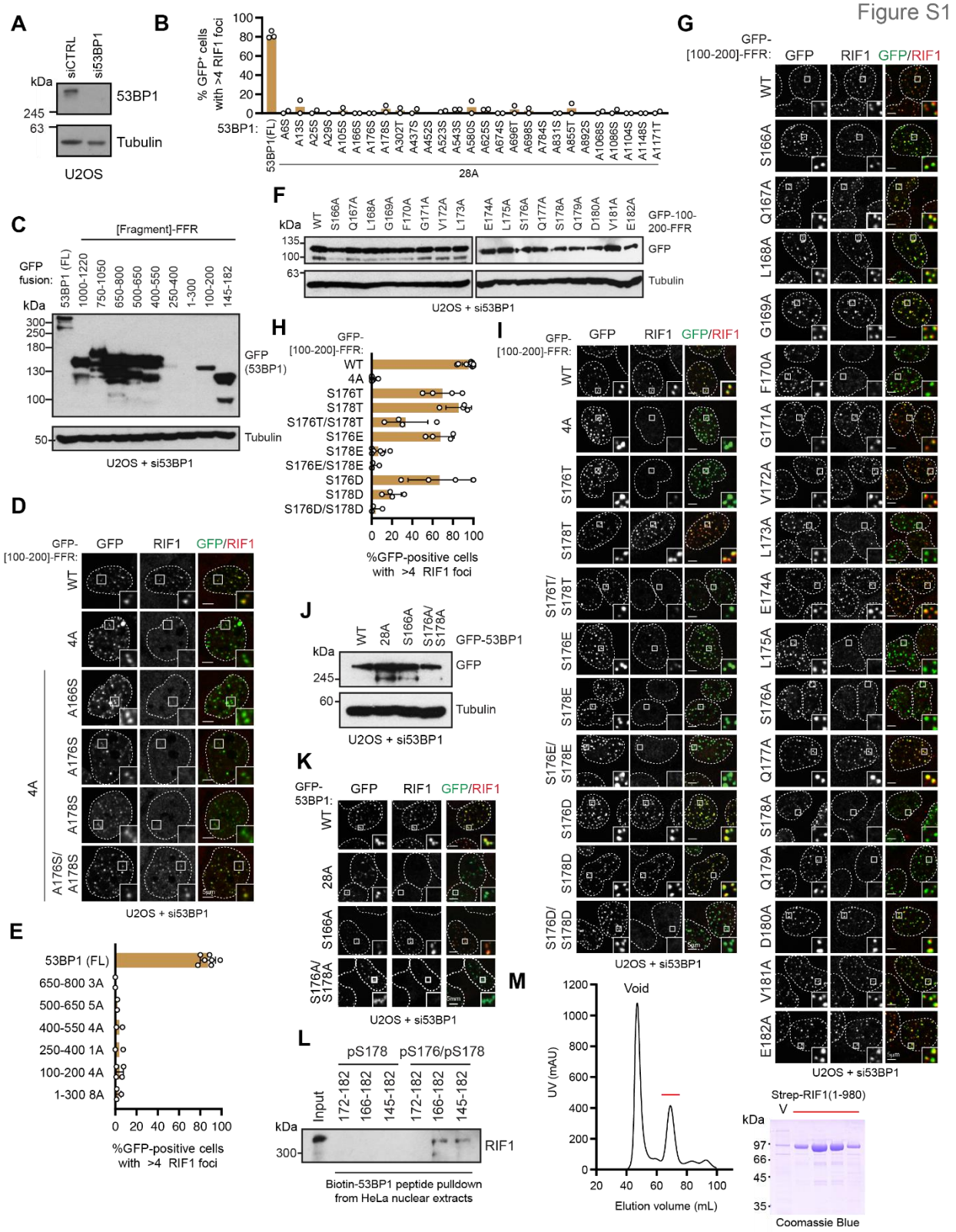
A
siCTRL
si53BP1
kDa
53BP1
245
63
Tubulin
U2OS
B
% GFP+ cells with >4 RIF1 foci
53BP1:
53BP1(FL)
28A
C
[Fragment]-FFR
GFP fusion:
53BP1 (FL)
kDa
GFP (53BP1)
Tubulin
U2OS + si53BP1
D
GFP-[100-200]-FFR:
GFP
RIF1
GFP/RIF1
4A
U2OS + si53BP1
E
53BP1 (FL)
650-800 3A
500-650 5A
400-550 4A
250-400 1A
100-200 4A
1-300 8A
%GFP-positive cells with >4 RIF1 foci
F
GFP-100-200-FFR
GFP
Tubulin
U2OS + si53BP1
H
GFP-[100-200]-FFR:
%GFP-positive cells with >4 RIF1 foci
I
J
GFP-53BP1
U2OS + si53BP1
K
GFP-53BP1:
U2OS + si53BP1
L
pS178
pS176/pS178
Input
RIF1
Biotin-53BP1 peptide pulldown from HeLa nuclear extracts
M
Void
UV (mAU)
Elution volume (mL)
G
GFP-[100-200]-FFR:
U2OS + si53BP1
Strep-RIF1(1-980)
Coomassie Blue

Figure S1. RIF1 directly binds doubly-phosphorylated 53BP1 N-terminal motifs, related to Figure 1

(A) Immunoblotting of whole cell extracts of U2OS cells transfected with a non-targeting siRNA (siCTRL) or an siRNA targeting 53BP1. Tubulin was used as a loading control.

(B) U2OS cells transfected with siRNA targeting 53BP1 were subsequently transfected with plasmids encoding wild type (WT) 53BP1 or the indicated 53BP1^{28A} reversion mutant. RIF1 focus formation 1 h post-IR (10 Gy) was evaluated by immunofluorescence. N=3 (53BP1 FL), all else N=2.

(C) Immunoblotting of whole cell extracts of U2OS cells expressing truncated GFP-53BP1 variants shown in Figure 1B. Tubulin was used as a loading control.

(D) Representative micrographs of RIF1 IR-induced focus formation data shown in Figure 1C.

(E) Analysis of RIF1 IR-induced focus formation in U2OS cells expressing the indicated 53BP1 variants 1 h post-IR treatment (10 Gy). Bar length corresponds to mean ± s.d.; N=7 (53BP1 FL), N=4 (100-200 4A), N=3 (1-300 8A), all else N=2.

(F) Immunoblotting of whole cell extracts of U2OS cells expressing GFP-[100-200]-FFR variants shown in Figure 1D. Tubulin was used as a loading control.

(G) Representative micrographs of RIF1 IR-induced focus formation data shown in Figure 1D.

(H) Analysis of RIF1 IR-induced focus formation in U2OS cells expressing the indicated 53BP1 [100-200]-FFR mutants, 1h post-IR (10 Gy). Bar length corresponds to mean ± s.d.; N=10 (WT), N=6 (4A, S178E), N=3 (S176E/S178E, S176D/S178D), all else N=4.

(I) Representative micrographs of the RIF1 IR-induced focus formation data shown in (H).

(J) Immunoblotting of whole cell extracts of U2OS cells expressing the full-length GFP-53BP1 variants shown in Figure 1F. Tubulin was used as a loading control.

(K) Representative micrographs of the RIF1 IR-induced focus formation data shown in Figure 1F.

(L) Streptavidin pulldown assay using the indicated biotinylated 53BP1 phosphopeptides incubated with HeLa nuclear extracts. Bound proteins were analyzed by immunoblotting with a RIF1 antibody.

(M) Purification of RIF1(1-980) from insect cells by streptactin affinity pulldown and size exclusion chromatography. Left: Chromatogram from size exclusion chromatography of recombinant RIF1(1-980). Red line indicates the residues analyzed by Coomassie Blue SDS-PAGE (right). V indicates sample from void peak.

Figure S2

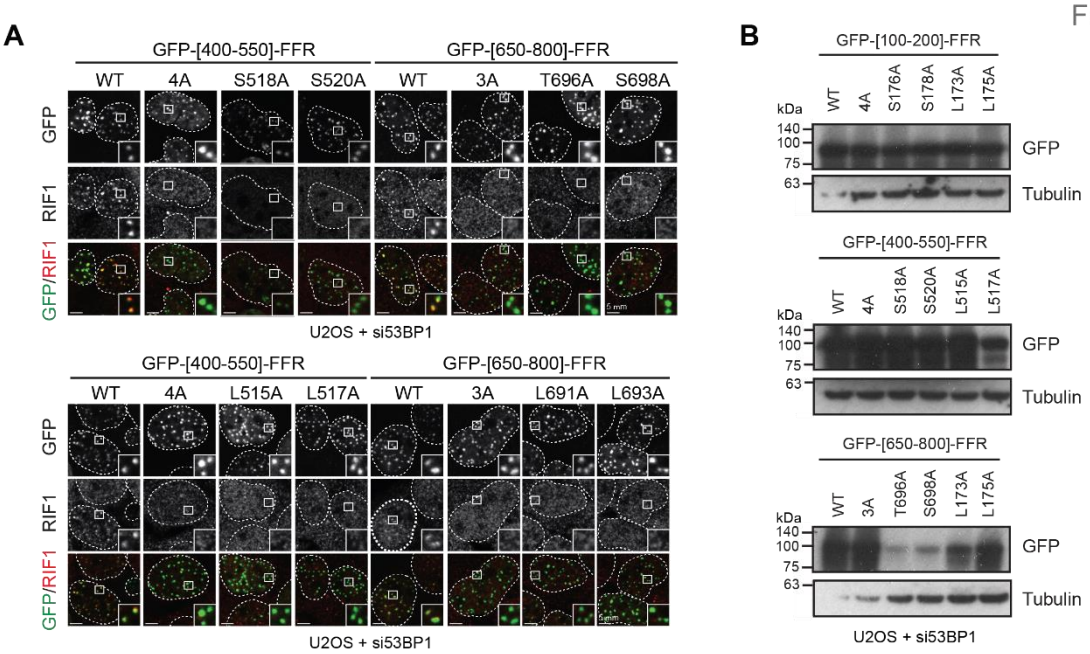
A
GFP-[400-550]-FFR
GFP-[650-800]-FFR
WT
4A
S518A
S520A
WT
3A
T696A
S698A
GFP
RIF1
GFP/RIF1
U2OS + si53BP1
GFP-[400-550]-FFR
GFP-[650-800]-FFR
WT
4A
L515A
L517A
WT
3A
L691A
L693A
GFP
RIF1
GFP/RIF1
U2OS + si53BP1
B
GFP-[100-200]-FFR
WT
4A
S176A
S178A
L173A
L175A
kDa
140
100
75
63
GFP
Tubulin
GFP-[400-550]-FFR
WT
4A
S518A
S520A
L515A
L517A
kDa
140
100
75
63
GFP
Tubulin
GFP-[650-800]-FFR
WT
3A
T696A
S698A
L173A
L175A
kDa
140
100
75
63
GFP
Tubulin
U2OS + si53BP1

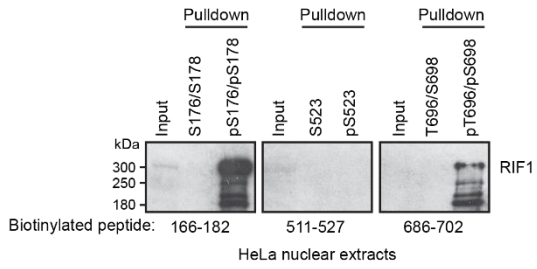
C
Pulldown
Pulldown
Pulldown
Input
S176/S178
pS176/pS178
Input
S523
pS523
Input
T696/S698
pT696/pS698
kDa
300
250
180
RIF1
Biotinylated peptide:
166-182
511-527
686-702
HeLa nuclear extracts

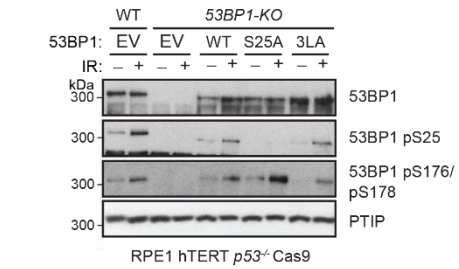
D
WT
53BP1-KO
53BP1:
EV
EV
WT
S25A
3LA
IR:
– + – + – + – + – +
kDa
300
53BP1
300
53BP1 pS25
300
53BP1 pS176/
pS178
300
PTIP
RPE1 hTERT p53-/- Cas9

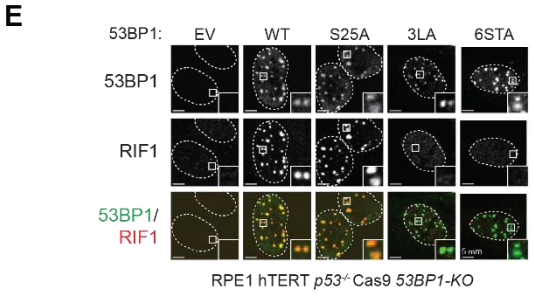
E
53BP1:
EV
WT
S25A
3LA
6STA
53BP1
RIF1
53BP1/
RIF1
RPE1 hTERT p53-/- Cas9 53BP1-KO

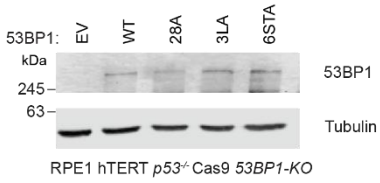
F
53BP1:
EV
WT
28A
3LA
6STA
kDa
245
63
53BP1
Tubulin
RPE1 hTERT p53-/- Cas9 53BP1-KO

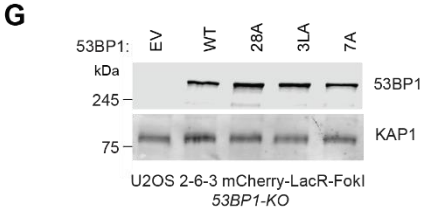
G
53BP1:
EV
WT
28A
3LA
7A
kDa
245
75
53BP1
KAP1
U2OS 2-6-3 mCherry-LacR-FokI
53BP1-KO

Figure S2. Characterization of additional RIF1-binding 53BP1 phosphopeptides, related to Figure 2

(A) Representative micrographs of the RIF1 IR-induced focus formation data shown in Figure 2B.

(B) Immunoblotting of whole cell extracts expressing the GFP-53BP1 variants used in (A). Tubulin was used as a loading control.

(C) Streptavidin pulldown assay using biotinylated 53BP1 phosphopeptides incubated with HeLa nuclear extracts. Bound proteins were analyzed by immunoblotting with a RIF1 antibody.

(D) Immunoblotting of whole cell extracts of wild-type (WT) or *53BP1-KO* RPE1-hTERT *p53*$^{-/-}$ Cas9 cells expressing the indicated 53BP1 variants harvested 1 h post-IR (10 Gy). EV, empty vector.

(E) Representative micrographs of the RIF1 IR-induced focus formation data shown in Figure 2E.

(F) Immunoblotting of whole cell extracts of RPE1-hTERT *p53*$^{-/-}$ Cas9 *53BP1-KO* cells expressing the indicated 53BP1 variants used in Figure 2E. Tubulin was used as a loading control.

(G) Immunoblotting of whole cell extracts U2OS 2-6-3 *53BP1-KO* cells expressing the indicated 53BP1 variants used in Figures 2G-H. KAP1 was used as a loading control.

Figure S3

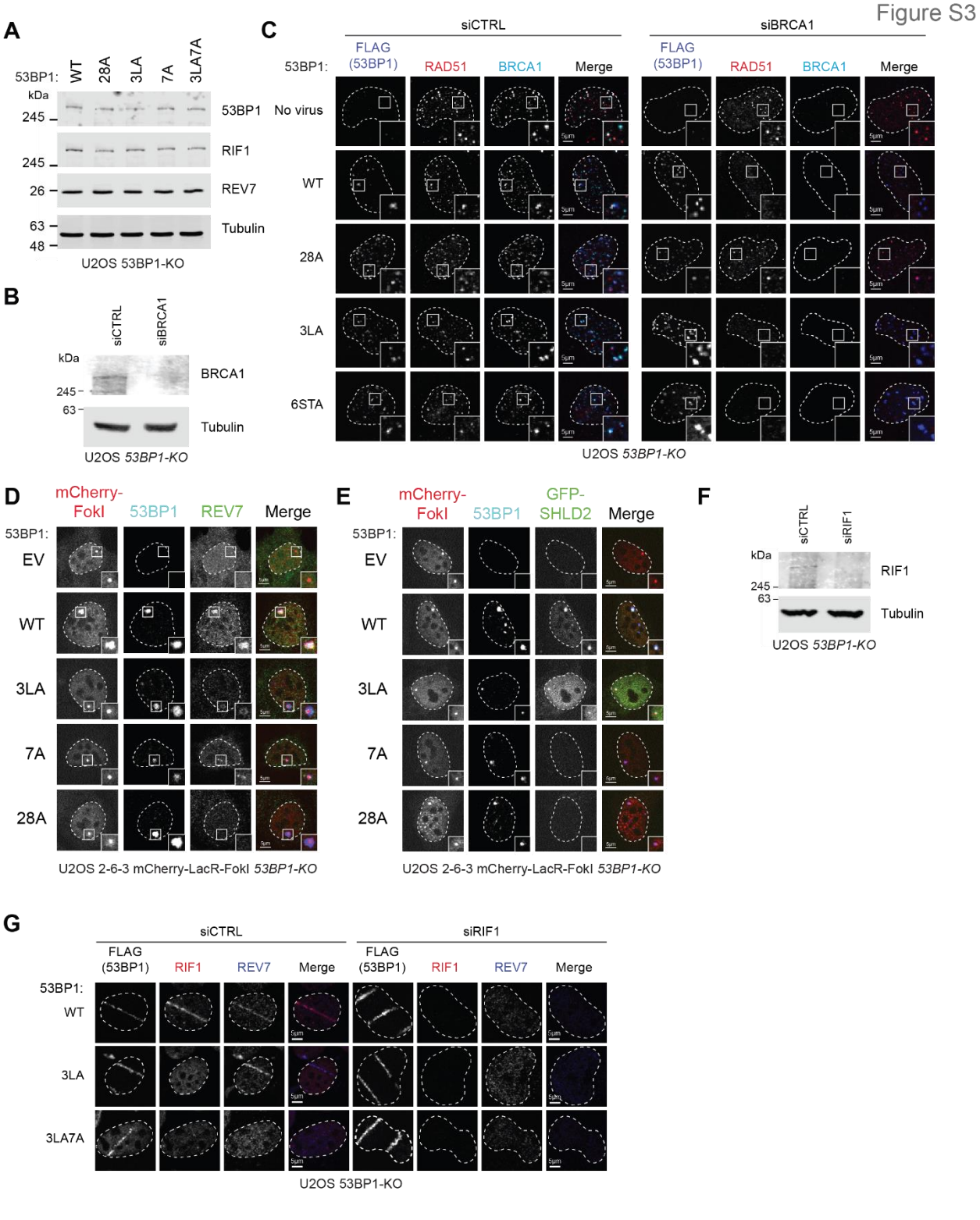
A
53BP1: WT 28A 3LA 7A 3LA7A
kDa
245
53BP1
245
RIF1
26
REV7
63
48
Tubulin
U2OS 53BP1-KO
B
siCTRL
siBRCA1
kDa
245
63
BRCA1
Tubulin
U2OS 53BP1-KO
C
siCTRL
siBRCA1
53BP1:
FLAG (53BP1)
RAD51
BRCA1
Merge
No virus
WT
28A
3LA
6STA
U2OS 53BP1-KO
D
mCherry-FokI
53BP1
REV7
Merge
53BP1:
EV
WT
3LA
7A
28A
U2OS 2-6-3 mCherry-LacR-FokI 53BP1-KO
E
mCherry-FokI
53BP1
GFP-SHLD2
Merge
53BP1:
EV
WT
3LA
7A
28A
U2OS 2-6-3 mCherry-LacR-FokI 53BP1-KO
F
siCTRL
siRIF1
kDa
245
63
RIF1
Tubulin
U2OS 53BP1-KO
G
siCTRL
siRIF1
FLAG (53BP1)
RIF1
REV7
Merge
53BP1:
WT
3LA
3LA7A
U2OS 53BP1-KO

Figure S3. Effect of disrupting RIF1-binding 53BP1 phosphopeptides on HR suppression and shieldin recruitment, related to Figure 3

(A) Immunoblotting of whole cell extracts of U2OS *53BP1-KO* cells infected with retroviruses encoding the indicated 53BP1 variants used in Figure 3A. Tubulin was used as a loading control.

(B) Immunoblotting of U2OS *53BP1-KO* cells transfected with non-targeting (siCTRL) or BRCA1-targeting (siBRCA1) siRNAs. Tubulin was used as a loading control.

(C) Representative micrographs of the RAD51 IR-induced focus formation data shown in Figure 3A.

(D) Representative micrographs of the REV7 and FokI-induced DSB colocalization data shown in Figure 3B. EV, empty vector.

(E) Representative micrographs of the GFP-SHLD2 and FokI-induced DSB colocalization data shown in Figure 3C.

(F) Immunoblotting of whole cell extracts of U2OS *53BP1-KO* cells transfected with non-targeting (siCTRL) or RIF1-targeting (siRIF1) siRNAs. Tubulin was used as a loading control.

(G) Representative micrographs of the REV7 colocalization with UV laser microirradiation tracks in RIF1-depleted cells shown in Figure 3G.

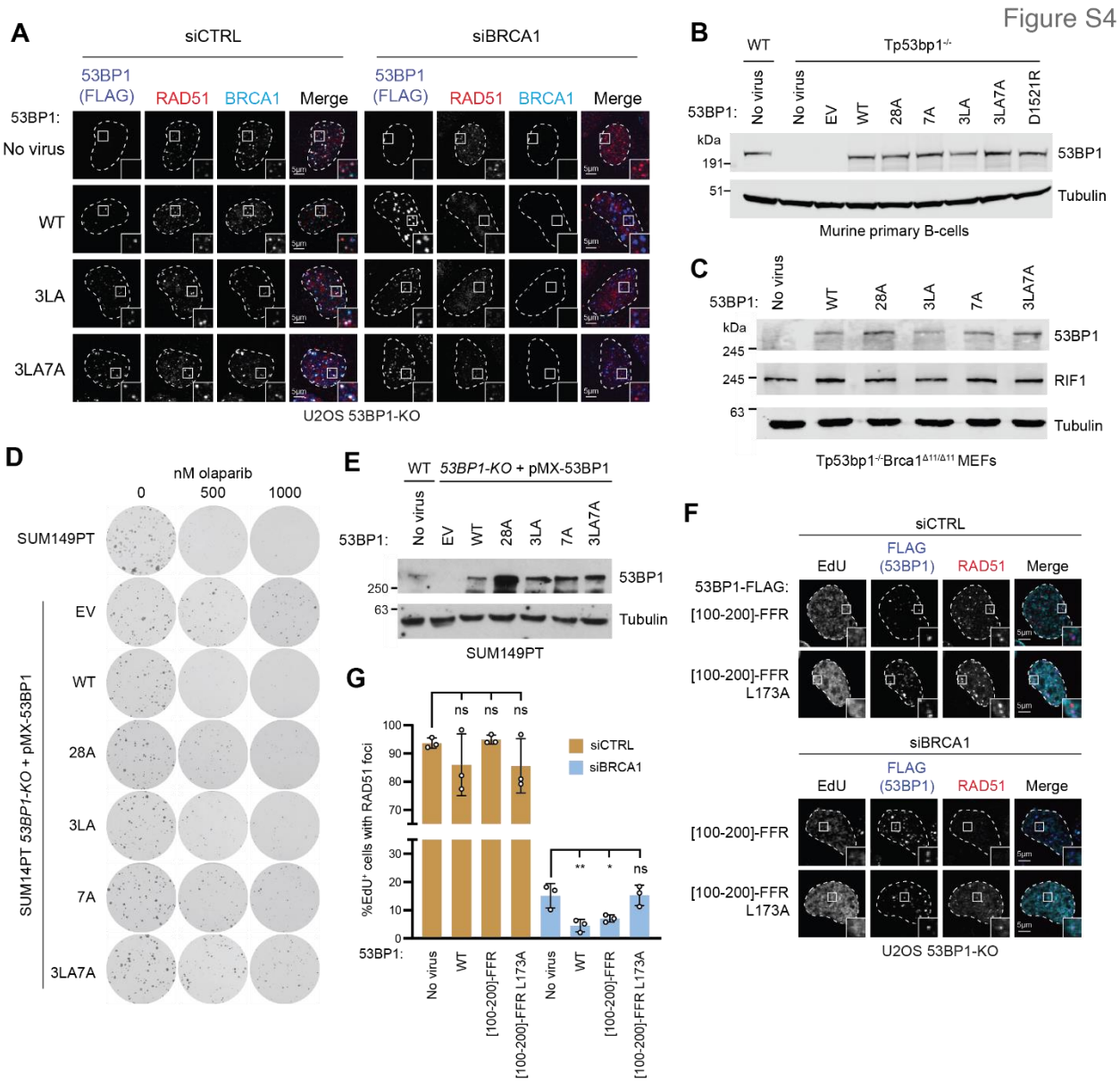

Figure S4. Effect of disrupting both RIF1 and shieldin recruitment on 53BP-mediated DNA repair, related to Figure 4.

(A) Representative micrographs of the RAD51 IR-induced focus formation data shown in Figure 4A.

(B) Immunoblotting of whole cell extracts of *Tp53bp1*$^{-/-}$ mouse splenic B-cells infected with retrovirus encoding the indicated 53BP1-FLAG constructs used in Figures 4B-C. Tubulin was used as a loading control.

(C) Immunoblotting of whole cell extracts of mouse embryonic fibroblasts isolated from *Tp53bp1*$^{-/-}$*Brca1*$^{\Delta 11/\Delta 11}$ mice infected with retroviruses encoding the indicated 53BP1-FLAG constructs used in Figures 4D-E. Tubulin was used as a loading control.

(D-E) Clonogenic survival assay of SUM149PT *53BP1-KO* cells infected with retrovirus encoding the indicated 53BP1-FLAG constructs 9 d after olaparib treatment. Whole cell extracts were analyzed by immunoblotting in (E), tubulin was used as a loading control. Quantitation is shown in Figure 4F. EV, empty vector.

(F-G) U2OS *53BP1-KO* cells were infected with retroviruses encoding the indicated 53BP1-FLAG constructs and transfected with a non-targeting siRNA (siCTRL) or an siRNA against BRCA1. Cells were treated with IR (5 Gy), and after 3.5 h were treated with EdU for 30 min. RAD51 foci in EdU-positive cells were then evaluated by immunofluorescence. Representative micrographs (F) and quantitation (G) are shown. Bar height corresponds to the mean ± s.d. N=3. * $p < 0.05$, ** $p < 0.01$. ns, not significant. Two-tailed unpaired t-tests were done relative to uninfected U2OS *53BP1-KO* cells.

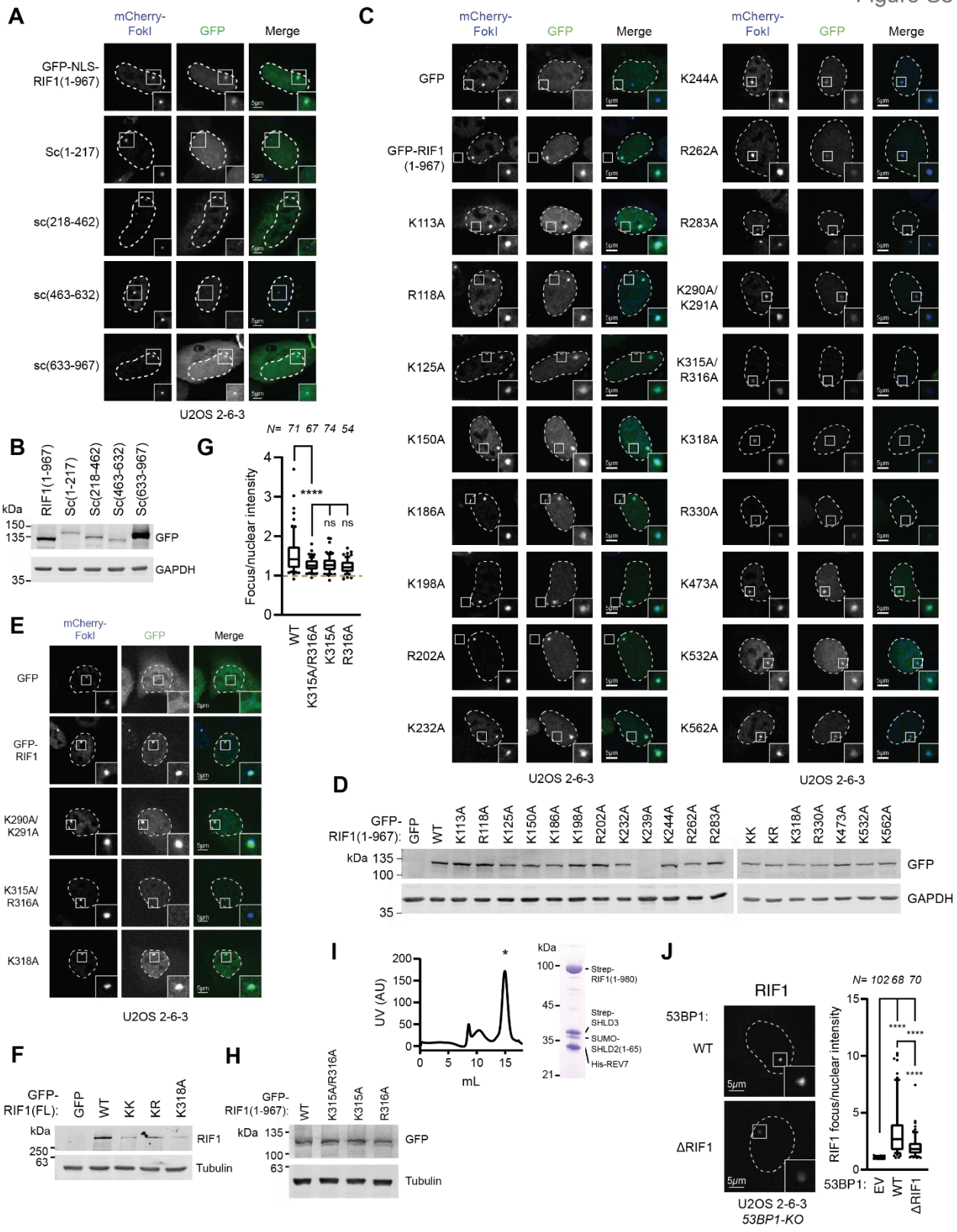
A
mCherry-FokI
GFP
Merge
GFP-NLS-RIF1(1-967)
Sc(1-217)
sc(218-462)
sc(463-632)
sc(633-967)
U2OS 2-6-3
B
RIF1(1-967)
Sc(1-217)
Sc(218-462)
Sc(463-632)
Sc(633-967)
kDa
150
135
GFP
35
GAPDH
G
N= 71 67 74 54
Focus/nuclear intensity
****
ns
ns
WT
K315A/R316A
K315A
R316A
C
GFP
GFP-RIF1 (1-967)
K113A
R118A
K125A
K150A
K186A
K198A
R202A
K232A
K244A
R262A
R283A
K290A/ K291A
K315A/ R316A
K318A
R330A
K473A
K532A
K562A
U2OS 2-6-3
E
GFP
GFP-RIF1
K290A/ K291A
K315A/ R316A
K318A
U2OS 2-6-3
D
GFP-RIF1(1-967):
GFP
WT
K113A
R118A
K125A
K150A
K186A
K198A
R202A
K232A
K239A
K244A
R262A
R283A
KK
KR
K318A
R330A
K473A
K532A
K562A
kDa
135
100
35
GFP
GAPDH
F
GFP-RIF1(FL):
GFP
WT
KK
KR
K318A
kDa
250
63
RIF1
Tubulin
H
GFP-RIF1(1-967):
WT
K315A/R316A
K315A
R316A
kDa
135
100
63
GFP
Tubulin
I
UV (AU)
200
150
100
50
0
0
5
10
15
mL
*
kDa
100
45
35
21
Strep-RIF1(1-980)
Strep-SHLD3
SUMO-SHLD2(1-65)
His-REV7
J
RIF1
53BP1:
WT
ΔRIF1
5μm
U2OS 2-6-3
53BP1-KO
N= 102 68 70
RIF1 focus/nuclear intensity
15
10
5
0
****
****
****
53BP1:
EV
WT
ΔRIF1

Figure S5. RIF1 recruitment requires conserved basic residues, related to Figure 5

(A) Representative micrographs of the GFP-RIF1 and FokI-induced DSB colocalization data shown in Figure 5B.

(B) Immunoblotting of whole cell extracts of U2OS 2-6-3 cells expressing the indicated GFP-RIF1(1-967) variants containing segments substituted with ScRif1 used in Figure 5B. GAPDH was used as a loading control.

(C-D) Representative micrographs of the GFP-RIF1(1-967) and FokI-induced DSB colocalization data shown in Figure 5C are shown in (C). Immunoblotting of whole cell extracts of U2OS 2-6-3 cells expressing the indicated GFP-RIF1(1-967) variants is shown in (D). GAPDH was used as a loading control. KK, K290A/K291A; KR, K315A/R316A.

(E) Representative micrographs of the GFP-RIF1 and FokI-DSB colocalization data shown in Figure 5D.

(F) Immunoblotting of whole cell extracts of U2OS 2-6-3 cells expressing the indicated GFP-RIF1 variants. Tubulin was used as a loading control. KK, K290A/K291A; KR, K315A/R316A.

(G) Quantitation of colocalization between the indicated GFP-RIF1(1-967) variants and FokI-induced DSBs in U2OS 2-6-3 evaluated by immunofluorescence. Fluorescence intensity relative to nuclear signal is shown. Data from three biological replicates are presented as boxplots. Whiskers indicate 10^{th} and 90^{th} percentiles, while the box indicate median and 25^{th} and 75^{th} percentiles.

(H) Immunoblotting of whole cell extracts of U2OS 2-6-3 cells expressing the indicated GFP-RIF1(1-967) variants used in (G). Tubulin was used as a loading control.

(I) Size exclusion chromatography of purified Strep-RIF1(1-980)-Strep-SHLD3-SUMO-SHLD2(1-65)-His-REV7. Peak marked by the asterisk was analyzed by Coomassie-stained SDS-PAGE analysis and shown.

(J) Left, representative micrographs of U2OS 2-6-3 *53BP1-KO* cells transfected with the indicated 53BP1 constructs and evaluated for RIF1 colocalization with FokI-induced DSBs. Right, quantitation of RIF1 colocalization with FokI-induced DSBs. Fluorescence intensity

relative to nuclear signal is shown. Data is presented as boxplots. Whiskers indicate 10^{th} and 90^{th} percentiles, while the box indicate median and 25^{th} and 75^{th} percentiles.

Table S1. Validation of detected crosslinks using REV7-SHLD3-SHLD2 structure (6KTO), related to Figure 4G.

REV7-SHLD3 interlinks			
REV7	**SHLD3**	**Distance to C-REV7 (Å)**	**Distance to O-REV7 (Å)**
209	25	49.0	14.1
44	25	41.1	33.4
90	25	56.2	11.7
162	25	56.6	29.7
190	25	29.2	45.3
198	25	33.6	29.3
167	25	61.7	40.9
167	54	11.6	70.3
162	54	15.3	67.8

REV7-REV7 intralinks					
Residue 1	**Residue 2**	**Distance in C-REV7-C-REV7 (Å)**	**Distance in O-REV7-O-REV7 (Å)**	**Distance in C-REV7-O-REV7 (Å)**	**Distance in O-REV7-C-REV7 (Å)**
44	162	34.6	39.3	52.2	41.9
209	198	32.0	29.4	27.0	19.9
190	162	30.1	23.4	41.8	66.5
209	90	11.5	11.1	46.7	47.4
209	44	29.4	29.6	25.5	34.2
209	190	24.4	47.4	34.3	18.2
167	198	31.0	24.9	55.0	56.5
209	167	35.4	46.7	48.1	49.3
209	162	35.7	38.1	47.8	43.1
162	198	23.6	21.0	52.4	51.1
167	190	34.8	18.1	68.1	47.2

SHLD3-SHLD2 interlinks		
SHLD3	**SHLD2**	**Distance (Å)**
25	51	18.6

SHLD3-SHLD3 intralinks		
Residue 1	**Residue 2**	**Distance (Å)**
48	25	51.8
25	54	58.8

Short unresolved loops were modeled in using SwissModel. Highlighted cells show the shortest Cα-Cα distance